

## **Supplemental Materials**

### **Online Methods**

#### **Animal model**

Mice with cardiomyocyte-restricted low-level overexpression of long-chain acyl-CoA synthetase 1 (ACStg) and control littermates (WT) were originally on the FVB background<sup>1</sup>. We prepared a transgenic line on the C57BL6j background by backcrossing more than 8 generations. DRP1 floxed mice (Kind gift of Hiromi Sesaki, Johns Hopkins University, Baltimore MD) were used to generate cardiomyocyte-restricted heterozygous deletions of DRP1 (Mixed Background). Sod2 transgenic mice (FVB background) were a kind gift from Paul Epstein (University of Louisville, Louisville, KY) and Des1 +/- mice (C57BL6 background) were a kind gift of Scott Summers (University of Utah, Salt Lake City, UT). Animals were studied in accordance with protocols approved by the Institutional Animal Care and Use Committees of the University Utah and the Carver College of Medicine of the University of Iowa. All mice were housed at 22°C with free access to water and food (standard chow diet) with a light cycle of 12h light and 12h dark.

#### ***In vivo* cardiac function**

Echocardiography or left-ventricular (LV) catheterization was performed in a subset of the mice before respiration studies as described previously<sup>2</sup>. Mice were lightly anesthetized with isoflurane and imaged in the left lateral decubitus position with a linear 13-MHz probe (Vivid V echocardiograph; GE Healthcare, Tampa, FL). Cardiac dimensions and function were calculated from these digital images. Invasive LV hemodynamic measurements were performed with a temperature-calibrated 1.4-Fr micromanometer-tipped catheter (Millar Instruments, Houston, TX) inserted through the right carotid artery in mice anesthetized with choral hydrate (400 mg/kg) and analyzed as described by us previously.

#### ***In vivo* palmitate uptake**

*In vivo* palmitate uptake was measured by quantifying cardiac palmitate biodistribution of 1-<sup>11</sup>C-palmitate using small-animal positron emission tomography (PET) as described before <sup>3</sup>.

#### ***In vivo* MG132 administration**

10mg of MG132 (EMD Millipore, Billerica, MA) was dissolved in Corn Oil (Sigma-Aldrich, St, Louis, MO) by rotating 24hrs in room temperature. MG132 (10mg/kg body weight) was administered intraperitoneally twice, prior to euthanasia (- 18h and - 6h).

#### **Cardiomyocyte isolation**

Primary cultures of neonatal rat ventricular cardiomyocytes (NRVCs) were prepared from the ventricles of 3-5-day-old Wistar rats as described previously <sup>4</sup>. NRVCs were plated on type I collagen coated cover glass or culture plates and incubated with DMEM supplemented with BSA or palmitate-BSA. NRVCs were also infected with adenovirus expressing either Ad-GFP or Ad-DRP1K38E at 10 MOI. The CRP-DRP1-K38E adenovirus was a gift from Dr. Ruth Slack's laboratory, Ottawa, Canada <sup>5</sup>. After 12hr. of infection, NRVCs were incubated in DMEM or palmitate as described above.

#### **Mitochondrial fusion assay**

Mitochondrial fusion was investigated using the PEG fusion assay, as described before with minor modifications <sup>6</sup>. In brief, L6 myoblasts were infected with mitoGFP or mitoRFP (kind gifts from Dr. D. Chan) using retrovirus infection, and 25,000 cells expressing mitoGFP or mitoRFP were co-plated on 18mm coverslips in 6-well plates. Fusion was initiated by adding 300µl of 50% PEG 1500 (Roche, Indianapolis, IN) for 60s, followed by addition of 2ml DMEM and two more washing steps with DMEM. Cells were incubated with 1ml cycloheximide (30µg/ml) for 8 h, washed with 1X PBS, and fixed with 3.7% formaldehyde. Cells were viewed on a FluoView FV1000 confocal microscope (Olympus, Tokyo, Japan) at a magnification of 630x.

#### **Immunofluorescence**

Adult cardiomyocytes and neonatal rat ventricular cardiomyocytes were isolated as described before <sup>7</sup>. For mitochondrial staining of adult cardiomyocytes, cells were incubated in HEPES buffer (126mM NaCl, 4.4mM KCl, 1.0mM, MgCl<sub>2</sub>, 1.08mM CaCl<sub>2</sub>, 11mM dextrose, 0.5mM probenecid, 24mM HEPES, pH 7.4) containing 100nM of the fluorescent potential-dependent indicator, tetramethylrhodamine ethyl ester (TMRE; Molecular Probes, Eugene, OR), for 30min at 37°C. Cells were then placed into a glass-bottom perfusion chamber mounted on a Zeiss LSM 510 confocal microscope (Zeiss, Oberkochen, Germany), perfused with HEPES-buffer at 37°C, and viewed. For neonatal rat ventricular cardiomyocytes grown on coverslips, cells were washed in warm PBS, fixed in 4% paraformaldehyde in PBS (15 min in room temperature), then washed in PBS, permeabilized with 0.2% TritonX in PBS (10 min in room temperature) and blocked in blocking solution (5% BSA in PBS with 0.05% Tween20, 30 min in room temperature). Antibody labeling was performed by addition of 200 µl blocking solution with primary or secondary antibodies (1–5 µg/ml) and washing with PBS containing 0.05% Tween20. Samples were mounted in 40% glycerol/PBS on glass slides and sealed with clear nail polish. Images were acquired in an Olympus FV-1000 confocal microscope or a Zeiss LSM 710 confocal microscope. The following antibodies were used for immunohistochemistry: Tom20 (Santa Cruz Biotechnology, Dallas, TX, sc-11415), α-actinin (Sigma-Aldrich, A7811) and DRP1 (Novus Biologicals, Littleton, CO, h00010059-m01).

### **Mitochondrial function**

Mitochondrial oxygen consumption and ATP synthesis rates were measured in saponin permeabilized fibers using palmitoyl-carnitine/malate, pyruvate/malate, or glutamate/malate as substrate combinations, as described before <sup>8</sup>. Mitochondria were isolated by differential centrifugation, and oxygen consumption and ATP synthesis were measured using palmitoyl-carnitine/malate, pyruvate/malate, or glutamate/malate as substrate combinations, as described before <sup>9</sup>. OXPHOS complexes of isolated mitochondrial membranes were separated by blue-native gel electrophoresis, and complex activities were determined by in-gel staining assays, as described before <sup>9</sup>. Mitochondrial respiration rate in NRVCs were assessed using a Seahorse XFp Extracellular Flux Analyzer with the XFp Cell Mito Stress

Test Kit (Agilent, Santa Clara, CA). In brief, NRVCs were plated at 75,000 cells/well in a 24-well Seahorse assay plate and maintained for 48hrs with DMEM (5.5mM glucose, 10 $\mu$ M AraC, 5% FBS and 10% horse serum). 24hr before the assay, media was changed to DMEM (5.5mM glucose without AraC and serum) and subjected to Seahorse analysis with DMEM (5.5mM glucose) supplemented with BSA or fatty acid-conjugated BSA.

### **Mitochondrial membrane potential assay**

Mitochondrial membrane potential in NRVCs was measured by TMRM fluorescence intensity. In brief, NRVCs were plated at 50,000 cells/well in a 96-well black bottom dish. After palmitate stimulation, NRVCs were incubated with 10 $\mu$ M TMRM and 100 $\mu$ g/ml Hoechst for 30min at 37 $^{\circ}$ C. TMRM (540/580) and Hoechst (360/450) fluorescence intensity was measured by a SpectraMax3 plate reader (Molecular devices, Sunnyvale, California). The TMRM/Hoechst fluorescence ratio is used to determine the mitochondrial membrane potential.

### **ATP extraction and quantification**

ATP content in NRVCs was measured by an ENLITEN ATP Assay System Bioluminescence Detection Kit for ATP Measurement (Promega, Madison, WI). In brief, NRVCs were plated in a 96-well plate at a density of 50,000 cells/well. ATP was extracted with 50 $\mu$ l of TCA(1%)/EDTA(4mM) buffer.

### **Oxidative stress and superoxide production**

Mitochondrial H<sub>2</sub>O<sub>2</sub> production was measured with a fluorometric assay as described before<sup>8</sup>. Activity of aconitase was measured in isolated mitochondria using a spectrophotometric assay, and tissue ROS levels were measured by the conversion of nonfluorescent 2',7'-dichlorofluorescein-diacetate (DCFDA) to the highly fluorescent 2',7'-dichlorofluorescein (DCF), as described before<sup>8</sup>. In NRVCs, ROS levels were measured by CellRox Green reagent in accordance with the manufacturer's instructions (Thermo Fisher Scientific, Waltham, MA).

### **Quantification of mitochondrial dimension and volume density in 2D electron microscopy**

Samples for transmission electron microscopy were collected from left ventricular myocardium and fixed in 2.5% glutaraldehyde/1% paraformaldehyde, post-fixed in 2% osmium tetroxide, embedded in resin, and sectioned (80-100 nm thick), as described before<sup>8</sup>. Mitochondrial volume density and dimensions of their two-dimensional (2D) cross-section were analyzed by 2D-stereology in a blinded fashion using the point counting method<sup>8</sup>. Briefly, the image obtained at 3,000x magnification was overlaid with square grids. Mitochondrial volume density was calculated by a number of grids superimposed over mitochondria. Apparent mitochondria size was calculated as volume density / mitochondrial number.

### **Electron microscopy and tomography**

Hearts were Langendorff-perfused with Tyrode's solution containing 139mM NaCl, 3mM KCl, 17mM NaHCO<sub>3</sub>, 12mM D-(+)-glucose, 3mM CaCl<sub>2</sub> and 1mM MgCl<sub>2</sub> and cardioplegically arrested using a high-K<sup>+</sup> (25 mM) no-Ca<sup>2+</sup> modified Tyrode's solution. Cardioplegically arrested hearts were perfusion-fixed with iso-osmotic Karnovsky's fixative (2.4% sodium cacodylate, 0.75% paraformaldehyde, 0.75% glutaraldehyde; 300 mOsm). Tissue fragments were excised from the left ventricle and washed with 0.1 M sodium cacodylate, post-fixed in 1% OsO<sub>4</sub> for 1 h, dehydrated in graded acetone, and embedded in Epon-Araldite resin. Thin (80 nm) and semi-thick (280 nm) sections were placed on formvar-coated slot-grids, post stained with 2% aqueous uranyl acetate and Reynold's lead citrate. Colloidal gold particles (15 nm) were added to both surfaces of the semi-thick sections to serve as fiducial markers for tilt-series alignment. Preparations were imaged at the EMBL Heidelberg Electron Microscopy Core Facility using a Tecnai F30 electron microscope operating at 300 kV and Phillips CM120 BioTwin electron microscope operating at 120 kV. Images were captured on a 4K Eagle camera and SIS 1K KeenView, respectively.

For tomography, the SerialEM software package was used. The specimen holder was tilted from +60° to -60° at 1° intervals, followed by 90° rotation in the X-Y plane and a second round of acquisition (dual axis tilt). The images from each tilt-series were aligned by fiducial marker tracking and back-projected to generate two single full-thickness reconstructed volumes (tomograms), which were then combined to

generate a single high-resolution 3D reconstruction of the original partial cell volume. Isotropic voxel size was 1.25 nm. All tomograms were processed and analysed using IMOD software, which was also used to generate 3D models of relevant structures of interest<sup>10</sup>.

### **Immunoblot analysis**

Mitochondrial and cytosolic fractions were generated by homogenizing freshly excised hearts in homogenization buffer (20mM HEPES, 140mM KCl, 10mM EDTA, 5mM MgCl<sub>2</sub>, pH 7.4) with a Dounce tissue homogenizer, centrifuging the homogenate at 800 x g for 10min, and centrifuging the resulting supernatant at 8,000 x g for 10min. The supernatant is the cytosolic fraction. The pellet was washed by centrifugation at 10,000 x g and represents the mitochondrial fraction. Whole-cell extracts and mitochondrial membranes were prepared as described before<sup>11</sup>. Samples were loaded on SDS-PAGE, transferred to nitrocellulose or PVDF membranes, and incubated with specific antibodies. Bands were visualized using horseradish peroxidase-conjugated secondary antibodies and the ECL detection system (GE Healthcare, Piscataway, NJ), or fluorophore-conjugated secondary antibodies and the Odyssey fluorescence detection system (Li-Cor Biosciences, Alpharetta, GA). The following antibodies were used for immunoblotting: ACSL1 (Cell Signaling Technology, Boston, MA, #4047), phospho-ERK1/2 (Cell Signaling Technology, #9101), phospho-SAPK/JNK (Cell Signaling Technology, #9251), DRP1 pS616 (Cell Signaling Technology, #3455), DRP1 pS637 (Cell Signaling Technology, #6319), DRP1 (Novus Biologicals, h00010059-m01), 4-Hydroxyneonal (4HNE) (Abcam, Cambridge, MA, ab46545), Mitofusin 1 (Abcam, ab57602), OPA1 (BD Biosciences, San Jose, CA, #612606), Mitofusin 2 (Sigma-Aldrich, M6319), Fis1 (Enzo Life Sciences, Farmingdale, NY, ALX-210-1037-0100), MnSOD (Enzo Life Sciences, ADI-SOD-110-D).

### **Cardiac mitochondrial lipid analysis**

For mass spectrometry sample preparation, tissue pieces were homogenized with a glass on glass homogenizer in PBS and lipids extracted according to a modified Bligh and Dyer method<sup>12, 13</sup> using 1,000 nmol tetramyristal cardiolipin as an internal

standard (Avanti Polar Lipids). Cardiolipin was quantified using our previously published methods<sup>12</sup> using liquid chromatography coupled to electrospray ionization mass spectrometry in an API 4000 mass spectrometer.

### **Statistical analysis**

Results are presented as means  $\pm$  SEM. Data were analyzed using unpaired student T-tests. If more than two groups were compared, 1-way ANOVA was performed, and significance was assessed using Fisher's protected least significance difference test. For T-tests and ANOVA, the Graphpad and Statplus software package was used (SAS Institute, Cary, NC). For all statistical analyses, significant difference was accepted when  $P < 0.05$ .

1. Chiu HC, Kovacs A, Ford DA, Hsu FF, Garcia R, Herrero P, Saffitz JE and Schaffer JE. A novel mouse model of lipotoxic cardiomyopathy. *J Clin Invest*. 2001;107:813-22.
2. Hu P, Zhang D, Swenson L, Chakrabarti G, Abel ED and Litwin SE. Minimally invasive aortic banding in mice: effects of altered cardiomyocyte insulin signaling during pressure overload. *Am J Physiol Heart Circ Physiol*. 2003;285:H1261-9.

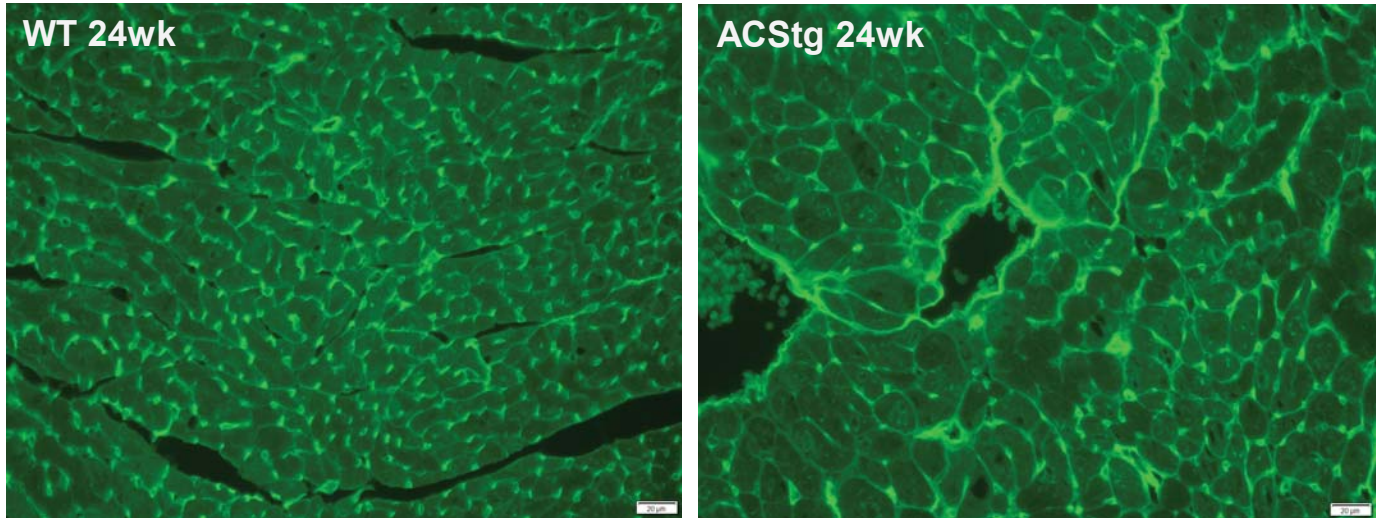
3. Chiu HC, Kovacs A, Blanton RM, Han X, Courtois M, Weinheimer CJ, Yamada KA, Brunet S, Xu H, Nerbonne JM, Welch MJ, Fettig NM, Sharp TL, Sambandam N, Olson KM, Ory DS and Schaffer JE. Transgenic expression of fatty acid transport protein 1 in the heart causes lipotoxic cardiomyopathy. *Circ Res.* 2005;96:225-33.
4. Chien KR, Sen A, Reynolds R, Chang A, Kim Y, Gunn MD, Buja LM and Willerson JT. Release of arachidonate from membrane phospholipids in cultured neonatal rat myocardial cells during adenosine triphosphate depletion. Correlation with the progression of cell injury. *J Clin Invest.* 1985;75:1770-80.
5. Germain M, Mathai JP, McBride HM and Shore GC. Endoplasmic reticulum BIK initiates DRP1-regulated remodelling of mitochondrial cristae during apoptosis. *EMBO J.* 2005;24:1546-56.
6. Chen H, Detmer SA, Ewald AJ, Griffin EE, Fraser SE and Chan DC. Mitofusins Mfn1 and Mfn2 coordinately regulate mitochondrial fusion and are essential for embryonic development. *J Cell Biol.* 2003;160:189-200.



7. Mazumder PK, O'Neill BT, Roberts MW, Buchanan J, Yun UJ, Cooksey RC, Boudina S and Abel ED. Impaired cardiac efficiency and increased fatty acid oxidation in insulin-resistant ob/ob mouse hearts. *Diabetes*. 2004;53:2366-74.
8. Bugger H, Boudina S, Hu XX, Tuinei J, Zaha VG, Theobald HA, Yun UJ, McQueen AP, Wayment B, Litwin SE and Abel ED. Type 1 diabetic akita mouse hearts are insulin sensitive but manifest structurally abnormal mitochondria that remain coupled despite increased uncoupling protein 3. *Diabetes*. 2008;57:2924-32.
9. Boudina S, Bugger H, Sena S, O'Neill BT, Zaha VG, Ilkun O, Wright JJ, Mazumder PK, Palfreyman E, Tidwell TJ, Theobald H, Khalimonchuk O, Wayment B, Sheng X, Rodnick KJ, Centini R, Chen D, Litwin SE, Weimer BE and Abel ED. Contribution of impaired myocardial insulin signaling to mitochondrial dysfunction and oxidative stress in the heart. *Circulation*. 2009;119:1272-83.
10. Rog-Zielinska EA, Johnston CM, O'Toole ET, Morpew M, Hoenger A and Kohl P. Electron tomography of rabbit cardiomyocyte three-dimensional ultrastructure. *Prog Biophys Mol Biol*. 2016;121:77-84.

11. Boudina S, Sena S, O'Neill BT, Tathireddy P, Young ME and Abel ED.  
Reduced mitochondrial oxidative capacity and increased mitochondrial uncoupling impair myocardial energetics in obesity. *Circulation*. 2005;112:2686-95.
12. Sparagna GC, Johnson CA, McCune SA, Moore RL and Murphy RC.  
Quantitation of cardiolipin molecular species in spontaneously hypertensive heart failure rats using electrospray ionization mass spectrometry. *J Lipid Res*. 2005;46:1196-204.
13. Bligh EG and Dyer WJ. A rapid method of total lipid extraction and purification. *Can J Biochem Physiol*. 1959;37:911-7.

## Online Figure I

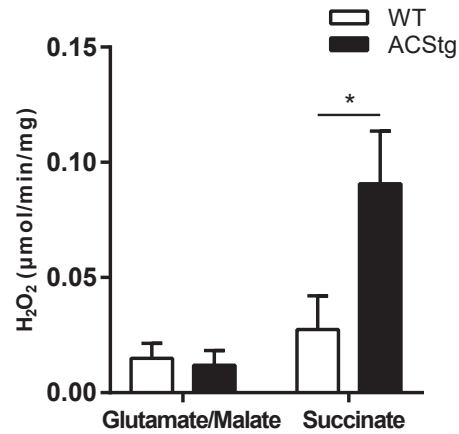


### Online Figure I

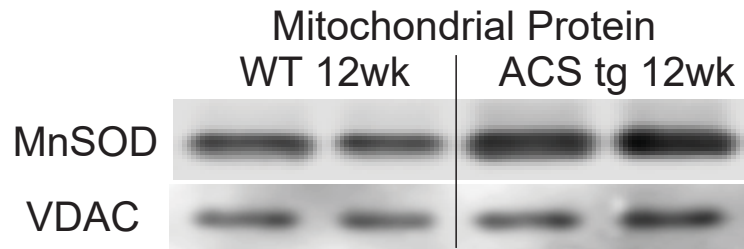
Representative images of wheat germ agglutinin staining of transverse heart sections obtained from 24-week-old ACStg mice and age-matched controls. Myocyte cross-sectional area were calculated from these images and presented in Figure 1H. Scale bars indicate 20 $\mu$ m.

**Online Figure II**

(A)



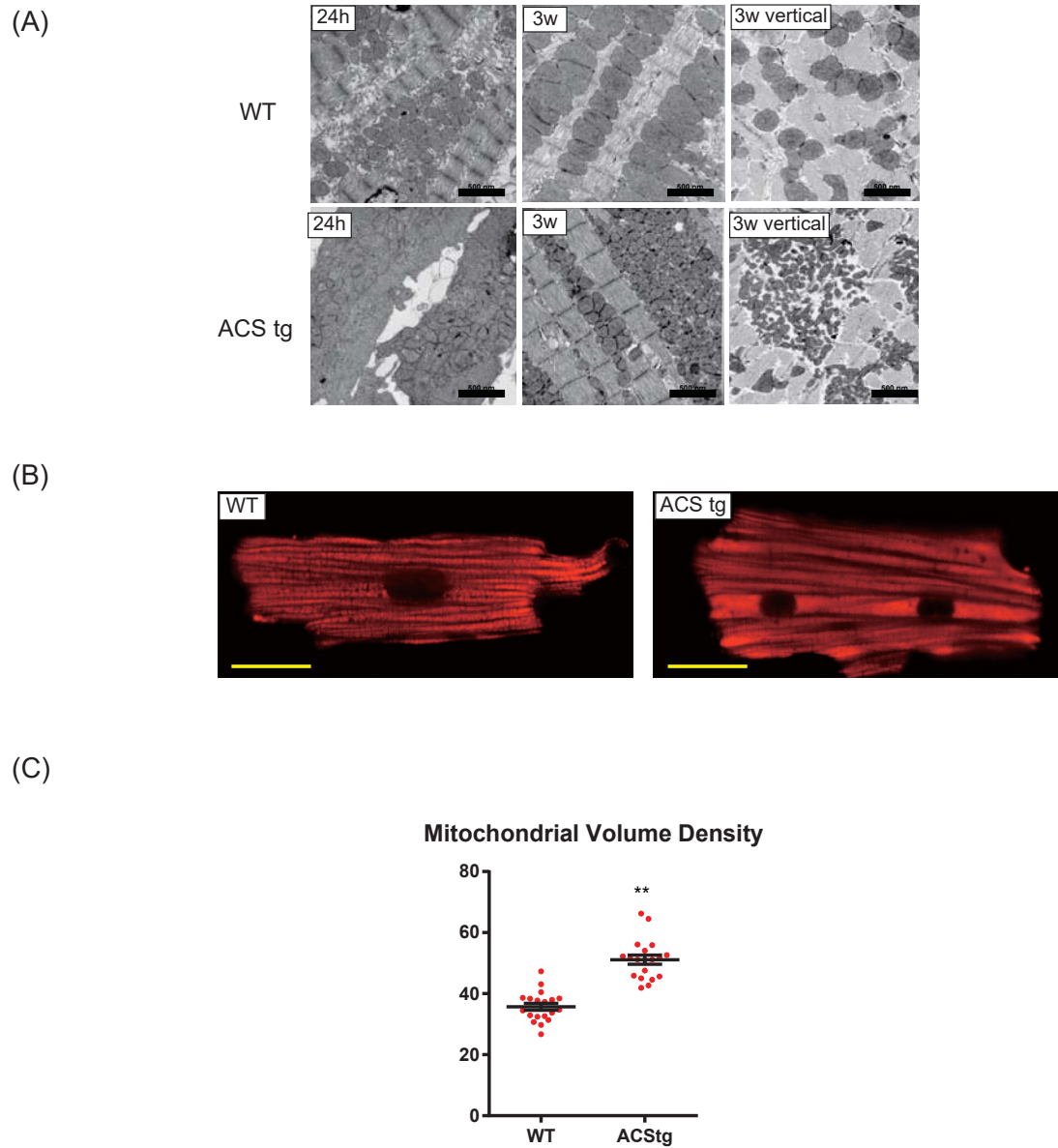
(B)



(A) H<sub>2</sub>O<sub>2</sub> production with glutamate or succinate as a substrate in mitochondria isolated from 12-week-old WT and ACStg hearts. n=3, \*, P<0.05 vs. WT

(B) Western blot of mitochondrial protein isolated from WT and ACStg hearts. Mitochondrial content of superoxide dismutase (SOD2 or MnSOD) and VDAC protein in 12-week-old WT and ACStg mice.

## Online Figure III



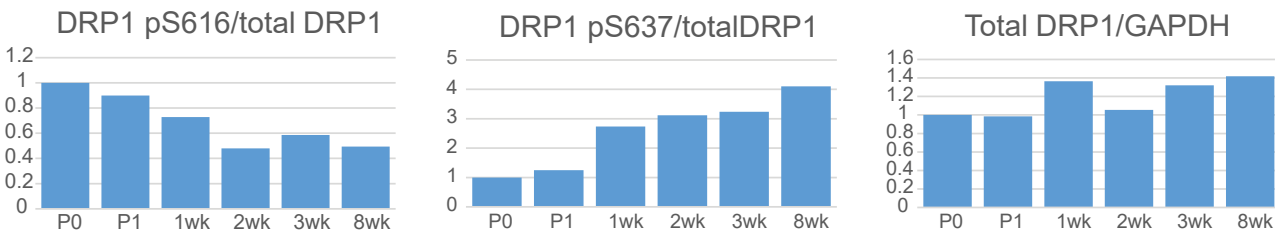
(A) Representative electron micrographs of longitudinal (24 hours, 3 weeks) or transverse (vertical) sections of WT and ACS tg hearts. Scale bars indicate 500nm.

(B) Representative confocal images of cardiomyocytes isolated from 12-week-old WT and ACS tg hearts, loaded with TMRE for 30 min. Scale bars indicate 20 $\mu$ m.

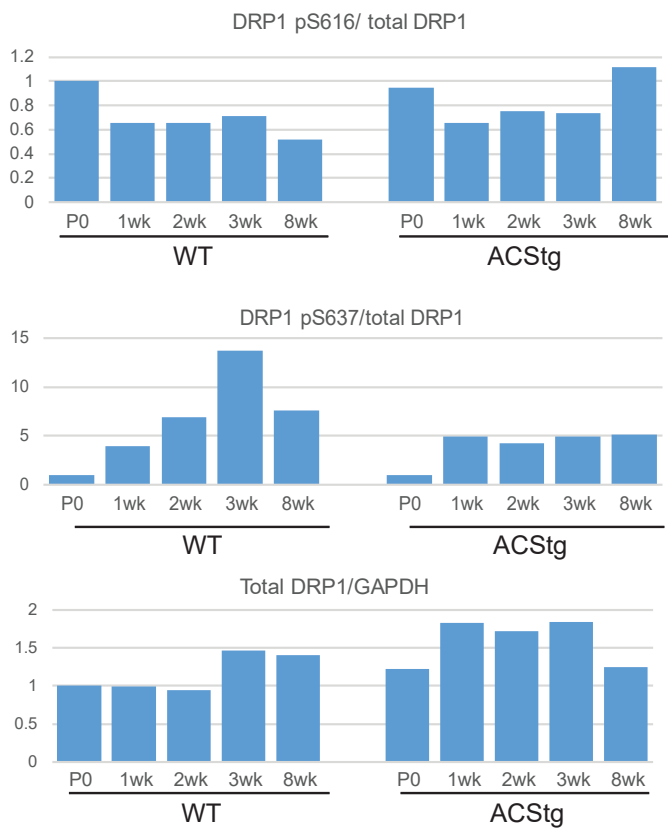
(C) Mitochondrial volume density was measured in 19 electron tomograms from 3 hearts per genotype; \*\* P < 0.01.

# Online Figure IV

(A)

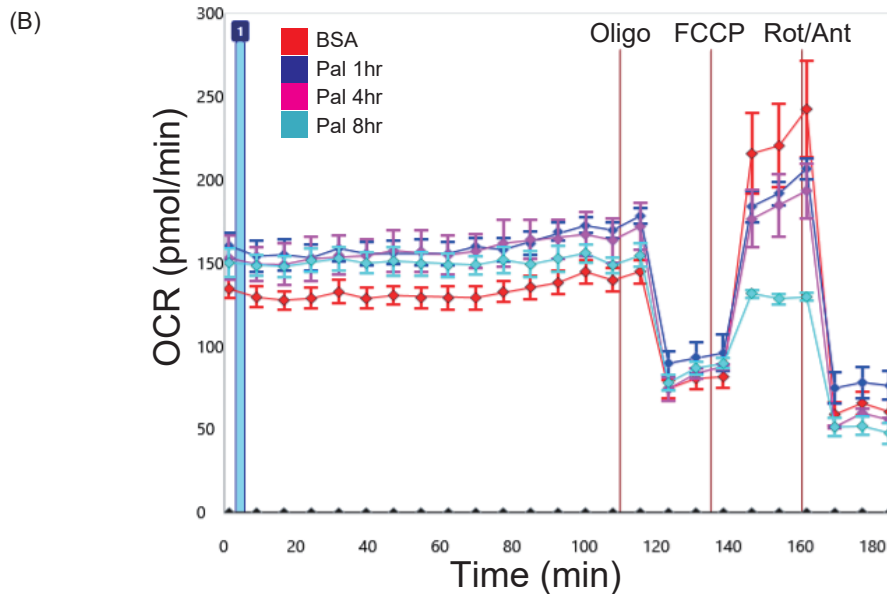
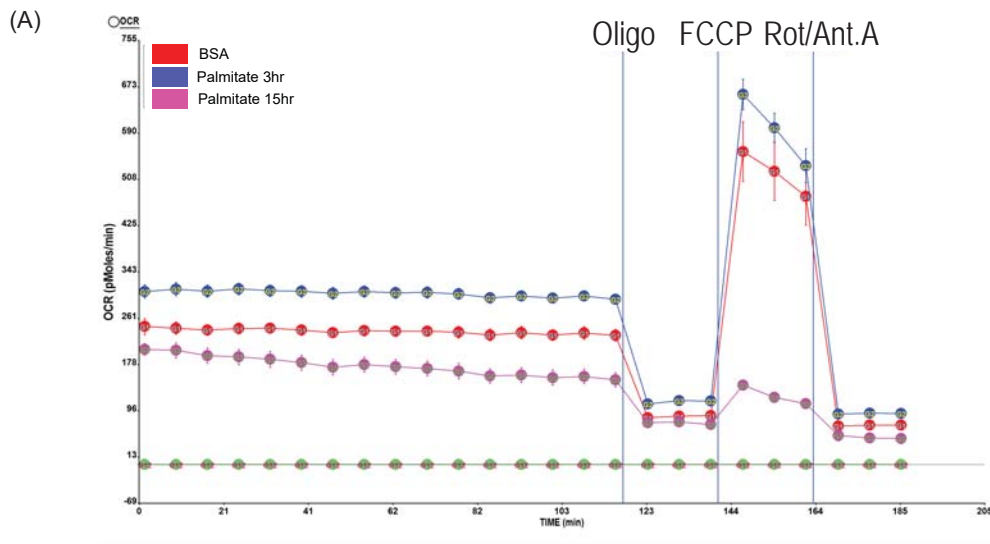


(B)



(A) Quantification of western blot presented in Figure 3G. Postnatal change of DRP1 phosphorylation in Wild-type whole heart homogenates.

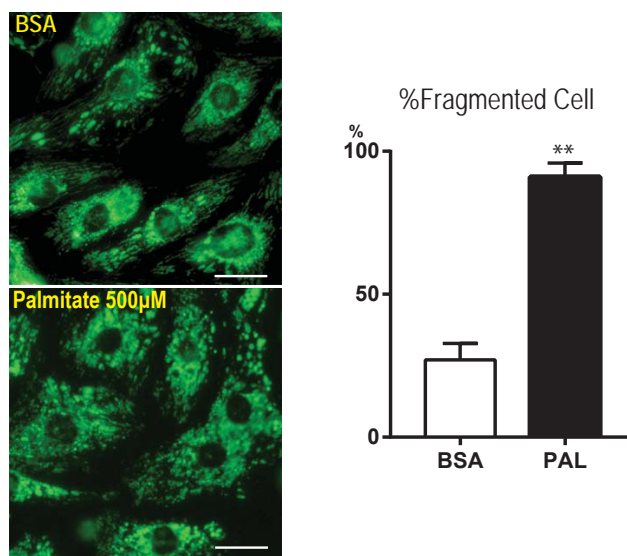
(B) Quantification of western blot presented in Figure 3H. Postnatal change of DRP1 phosphorylation was compared between Wild-type and ACS transgenic mouse hearts.



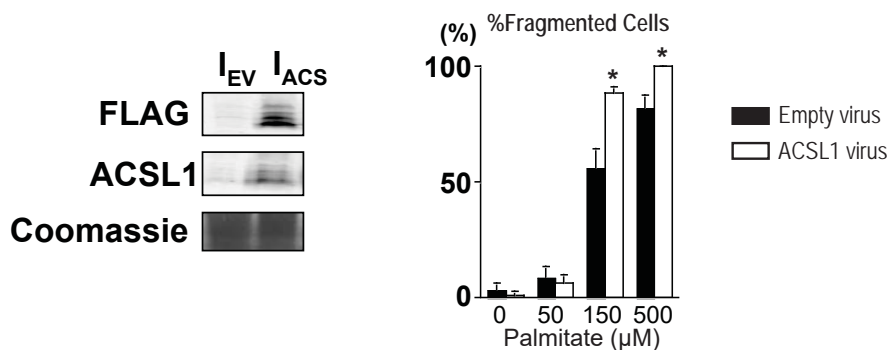
**(A)** NRVCs were pretreated with BSA or palmitate ( $500\mu\text{M}$ ) for 3h or 15h as indicated and oxygen consumption rate (OCR) was measured with the XF24 Extracellular Flux Analyzer (Seahorse Bioscience). Oligomycin ( $4\mu\text{M}$ ), FCCP ( $1\mu\text{M}$ ) + Antimycin A ( $1\mu\text{M}$ ) were sequentially added (indicated by lines). Short term palmitate treatment (3h) increased basal and maximum OCR. However, long term palmitate treatment (15h) decreased basal and maximum OCR.

**(B)** NRVCs were pre-treated with BSA or palmitate ( $500\mu\text{M}$ ) for 1h, 4h or 8h as indicated and OCR was measured with the XF24 Extracellular Flux Analyzer. Basal OCR was increased by palmitate treatment. Reduced maximum OCR was observed after 8h of palmitate treatment.

## Online Figure VI (A)



## (B)

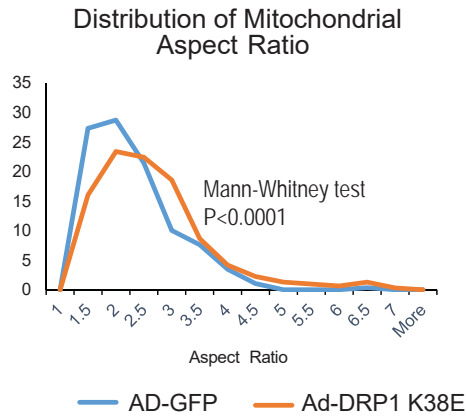


(A) Rat neonatal cardiomyocytes were incubated with culture medium supplemented with BSA or BSA conjugated palmitate (500 μM) for 12-hours. Mitochondria were stained with Mitotracker green according to the manufacturer's protocol. \*\*: P < 0.01 vs. WT, Scale bars indicate 20 μm.

(B) A representative Western blot for FLAG and ACSL1. I<sub>EV</sub> - lysate of L6 cells transfected with empty virus; I<sub>ACS</sub> - lysate of L6 cells transfected with ACSL1 virus. Cells infected with empty virus or ACSL1 virus were incubated in high-glucose DMEM + 10% FBS + 1% penicillin/streptomycin in the absence or presence of 500 μM palmitate for 5 hours. Cells were evaluated to contain a tubular or fragmented mitochondrial network, and cells with fragmented mitochondria were expressed as percentage of all viewed cells n=4, \* p<0.05 vs. Empty virus.



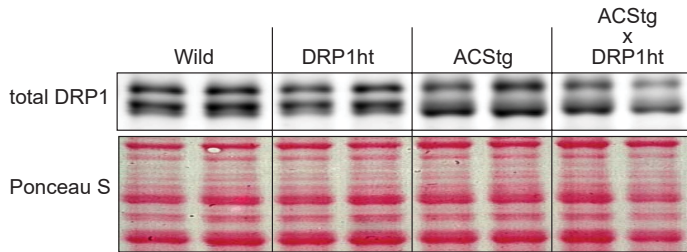
(A)



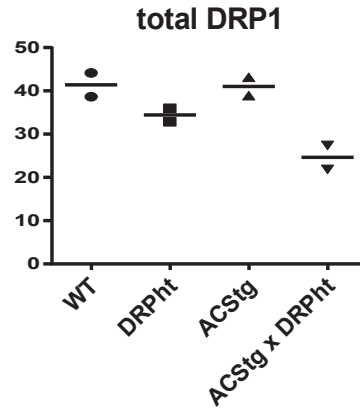
Mann-Whitney test of Mitochondria Aspect Ratio: Descriptive statistics

	Ad-GFP	Ad-DRP1 K38E
Number of values	222	272
Minimum	1.026	1.034
25% Percentile	1.445	1.668
Median	1.794	2.207
75% Percentile	2.405	2.829
Maximum	6.035	6.744
Mean	2.002	2.390
Std. Deviation	0.7332	0.9673
Std. Error of Mean	0.04921	0.05865
Lower 95% CI	1.905	2.274
Upper 95% CI	2.099	2.505
Mean ranks	211.7	276.7

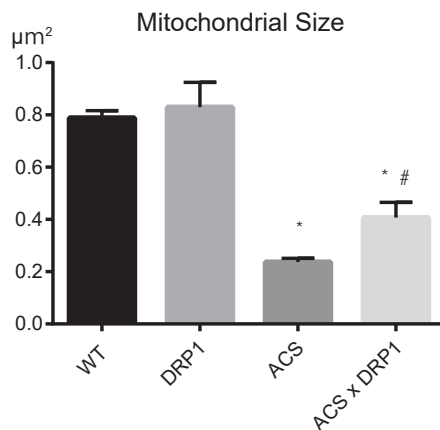
(B)



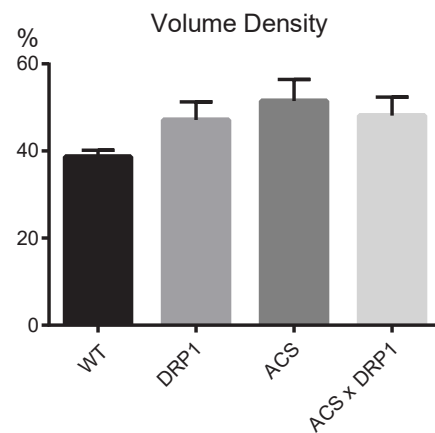
(C)



(D)



(E)



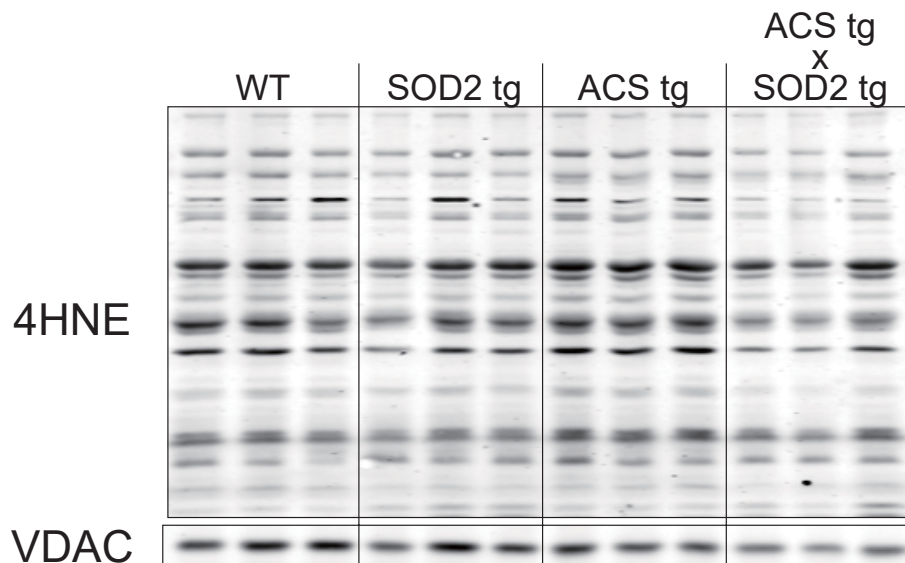
(A) Quantification of confocal images shown in Figure 6E. Mitochondrial aspect ratio was quantified by ImageJ as shown previously (Koopman et al., 2008).

(B-C) Western blot images of DRP1 protein content in whole heart lysates of Wild-type (WT), DRP1<sup>-/-</sup> (DRP1ht), ACStg and compound mutant mice (B) and densitometric quantification of the immunoblot (C).

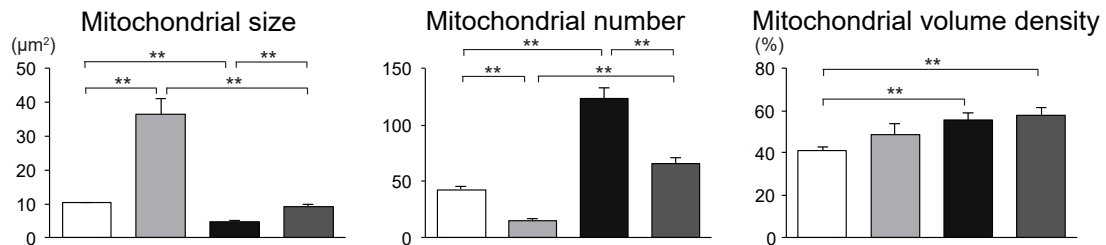
(D-E) Stereologic quantification of mitochondria size (D) and volume density (E) in WT, DRP1ht, ACStg and ACStg x

## Online Figure VIII

(A)



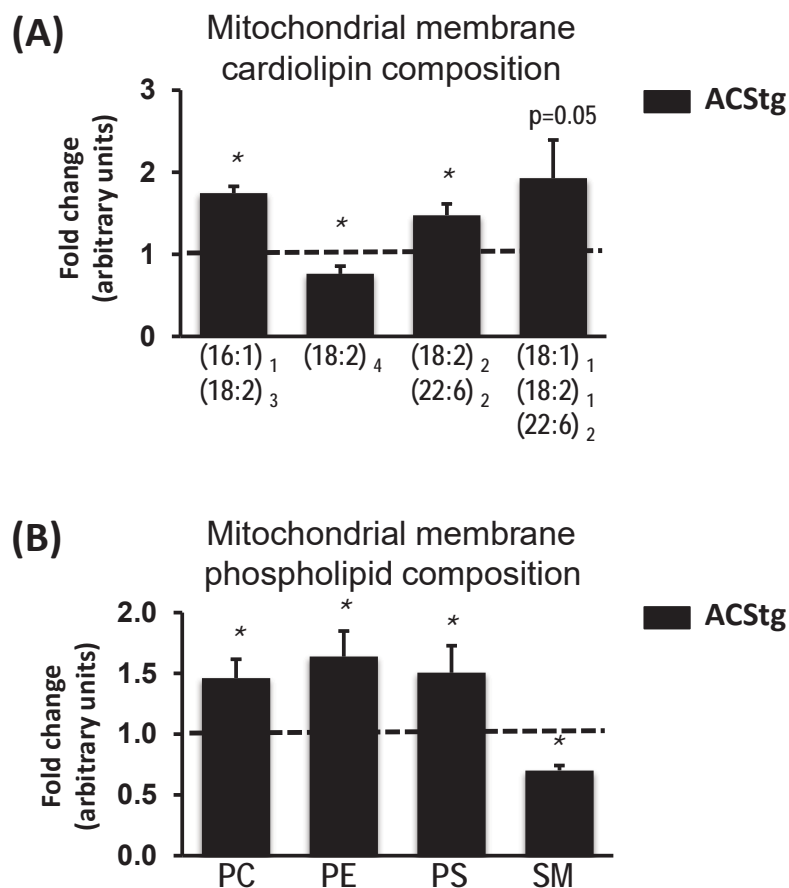
(B)



(A) Mitochondrial fractions were prepared from 12-week-old WT, SOD2tg, ACS tg and SOD2 x ACS double transgenic hearts and subjected to western blot for 4HNE

(B) Quantification of mitochondrial size obtained by blind counting of 2 equivalent sections from each of three separate hearts in each group depicted in Figure 6F \*\* P < 0.01.

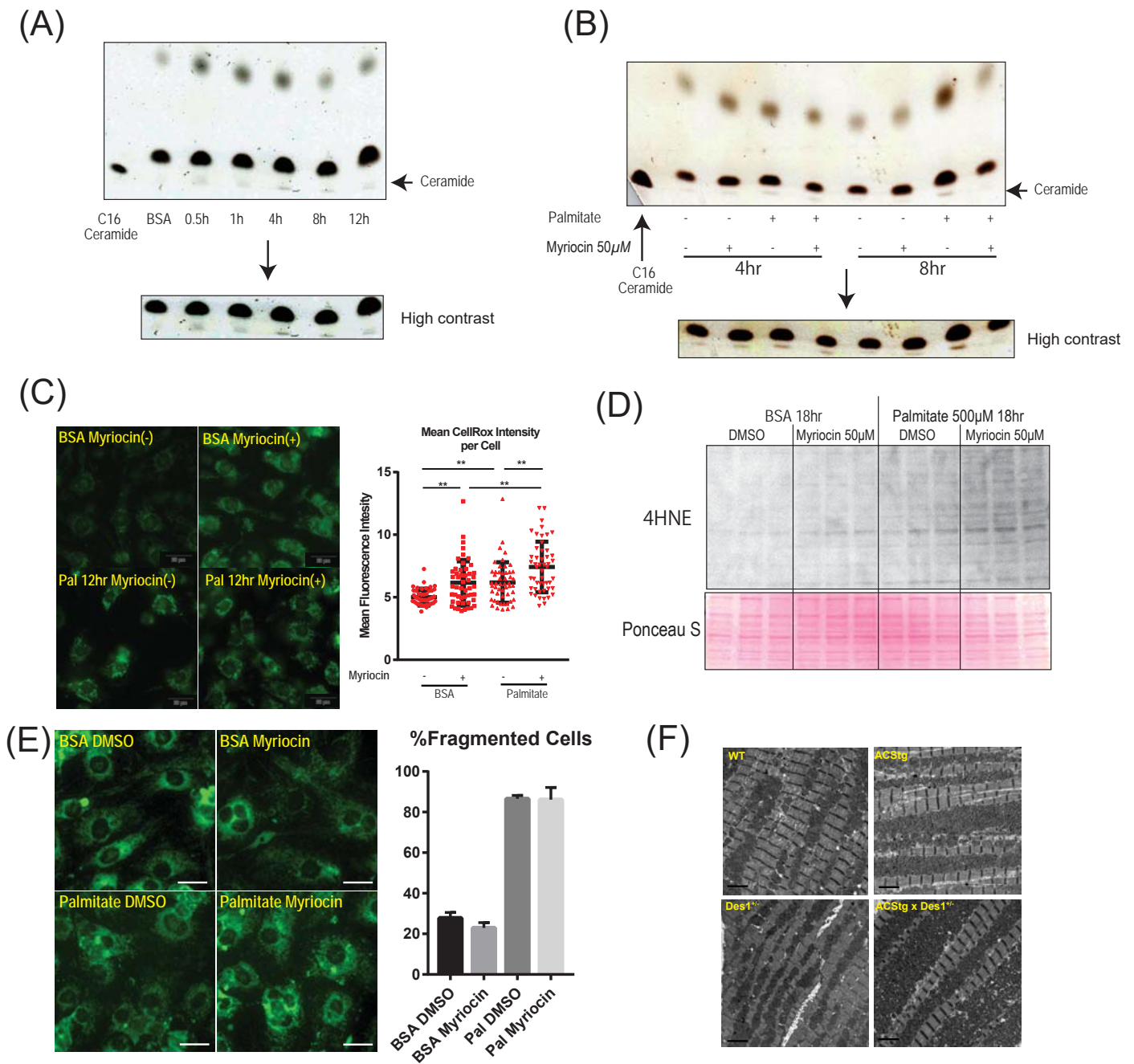
## Online Figure IX



**(A)** Cardiolipin composition in mitochondrial membranes isolated from 12 week-old WT and ACStg hearts measured by mass spectrometry (LC-MS/MS); n=6.

**(B)** Content of phosphatidylcholine (PC), phosphatidylethanolamine (PE), phosphatidylserine (PS), and sphingomyelin (SM) in mitochondrial membranes of 12 week-old WT and ACStg hearts measured by thin-layer chromatography; n=6.

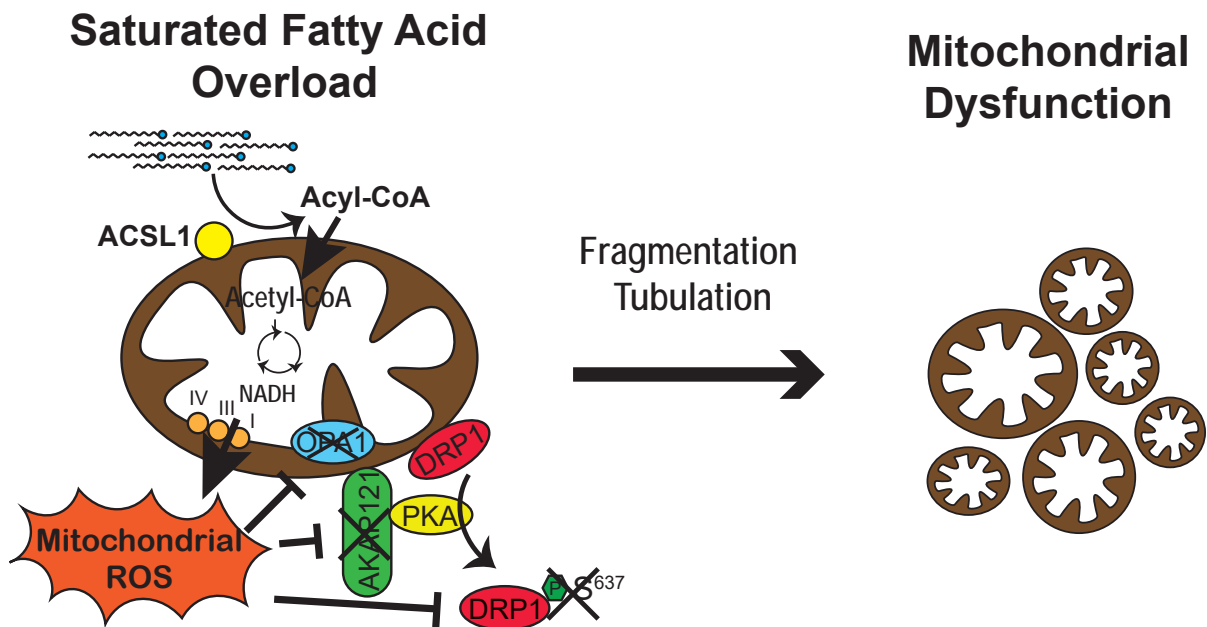
Data in (A) and (B) are expressed as fold change relative to WT, which was set to 1 (dashed line). \* p<0.05 vs. WT



**De novo ceramide synthesis inhibition does not rescue mitochondrial fragmentation after lipid overload**

**(A)** Lipids were extracted from NRVCs treated at the indicated time points after palmitate treatment and separated by thin layer chromatography (TLC). Lipids were visualized with sulfuric acid spray. Lane 1 is C16-ceramide control and arrow indicates the position of ceramide. **(B)** Lipid was extracted from NRVCs by chloroform/methanol (2:1) and separated by TLC. Myriocin inhibited the increase in ceramide level after palmitate treatment. **(C)** ROS production in NRVCs were visualised with CellROX green reagent (Thermo Fisher Scientific). ROS production was significantly increased after palmitate treatment. The blockade of ceramide de novo synthesis by myriocin enhanced ROS production. Scale bars indicate 20µm. **(D)** The synthesis of 4-HNE protein adducts were enhanced in myriocin treated groups. **(E)** Mitochondria were immunostained with an anti-Tom20 antibody. Representative images of NRVCs incubated in culture medium supplemented with BSA or 500µM palmitate in the presence or absence of 50µM myriocin, and quantification of fragmented mitochondria. Scale bars indicate 20µm. **(F)** Representative electron micrographs of longitudinal sections from 12-week-old wildtype (WT), ACStg, Des1<sup>-/-</sup> and ACStg x Des1<sup>-/-</sup> hearts. Inhibition of the ceramide de novo synthesis pathway could not rescue mitochondrial fragmentation and proliferation in ACStg hearts. Scale bars indicate 2µm.

# Cardiac Lipotoxicity



## Online Figure XI

Myocardial lipid overload, by saturated fatty acids, transiently increases mitochondrial respiration and ATP generation. Prolonged exposure to lipids increases mitochondrial ROS that modifies Drp1 and Opa1 to impair mitochondrial dynamics and function in the heart, contributing to cardiac hypertrophy and dysfunction.